ORIGINAL PAPER

Hydrothermal Synthesis of High-Quality Thiol-Stabilized $CdTe_xSe_{1-x}$ Alloyed Quantum Dots

Fanghong Yang · Ping Yang · Yongqiang Cao

Abstract Alloyed semiconductor quantum dots (QDs) enriched the synthetic routes for engineering materials with unique structural and optical properties. High-quality thiol-stabilized $CdTe_xSe_{1-x}$ alloyed QDs were synthesized through a facile and economic hydrothermal method at 120 °C, a relatively low temperature. These water-soluble QDs were prepared using different capping agents including 3-mercaptopropionic acid (MPA) and L-cysteine (L-Cys). The photoluminescence (PL) intensity and stability of L-Cys-capped $CdTe_xSe_{1-x}$ QDs were found to be higher than that of MPA-stabilized ones. The molar ratios of Se-to-Te upon preparation were adjusted for investigating the effect of composition on the properties of the resulting QDs. We also investigated the effect of the pH value of the reaction solution on the growth kinetics of the alloyed $CdTe_xSe_{1-x}$ QDs. The resulting $CdTe_xSe_{1-x}$ QDs were characterized by UV–vis absorbance and PL spectroscopy, powder X-ray diffraction, and transmission electron microscopy. Being coated with a CdS inorganic shell, the PL intensity and stability of the $CdTe_xSe_{1-x}$/CdS core-shell QDs were drastically enhanced, accompanied by the red-shift of the PL peak wavelength. Owing to the unique optical properties, the QDs hold great potential for application and have to be further exploited.

Keywords Quantum dots · Photoluminescence · CdTeSe · Semiconductor

F. Yang · P. Yang (✉) · Y. Cao
Shandong Provincial Key Laboratory of Preparation and Measurement of Building Materials, Key Laboratory of Inorganic Functional Materials of Shandong Universities, 250022 Jinan, People's Republic of China
e-mail: mse_yangp@ujn.edu.cn

F. Yang · P. Yang · Y. Cao
School of Material Science and Engineering, University of Jinan, 250022 Jinan, People's Republic of China

Introduction

Due to excellent optical properties, for example, size-tunable, narrow and symmetric emission spectra, high photoluminescence (PL) quantum yields (QYs), broad absorption spectra, and high photo stability, semiconductor quantum dots (QDs) have been extensively studied in the past two decades [1–4]. Recent years, the rapid progress of preparation techniques for semiconductor QDs has enabled the design of various sophisticated nanostructures, such as type I, type II, and alloyed QDs [5–8]. CdSe/ZnS core-shell QDs (type I), for example, can exhibit brighter and more stable emission when compared with bare CdSe cores. These QDs hold great potential for applications in optoelectronic devices, biological labeling, building blocks of superstructures [9–11], and so on.

These core-shell and alloyed QDs have different optical and electrical properties. In the case of type I QDs such as CdTe/ZnS QDs, the effective band gaps of the core-shell QDs are mostly governed by the size and composition of the core materials, as electrons and holes are dwell mostly in the core [12]. That means type I hetero structures are grown by encapsulation of the core having a narrow band gap with a shell having a wider band gap. In type II hetero structures, the conduction and valence band levels of the cores are offset from those in the shells [13]. Hence, the electrons and holes are located separately in the shells and cores, respectively. Alloyed semiconductor QDs enriched the synthetic routes for engineering materials with excellent optical and structural properties. Particularly, the effective band gap of the alloyed QDs can be adjusted, not only by the size of the QDs but also by the composition and degree of the alloying [14, 15]. The progress in preparation techniques has enabled the synthesis of various alloyed QDs, delivering either in water ($Cd_xHg_{1-x}S$ [16], $Cd_xHg_{1-x}Te$ [17]) or organic solvents ($Zn_xCd_{1-x}S$ [18] and $Cd_xZn_{1-x}Se$ [19]). For biological application, the QDs synthesized in organic phase have to be

transferred into aqueous phase from organic solvents to enable their applications, which always involve a surface-modification process. However, this process has several invincible drawbacks such as limited stability and low PL QYs. Thus, it would be more advantageous if QDs with water-soluble properties can be synthesized directly in aqueous phase.

Currently the synthesis of alloyed QDs is mainly in organic phase at high temperature, which usually involves complex manipulation at high temperature and toxic environment. The synthesis of water-soluble QDs in aqueous phase can be achieved by several approaches, including refluxing approach, hydrothermal method, and microwave-assisted synthesis. Compared with organic routes, an aqueous-based synthesis has many advantages, such as simplicity, low-cost, repeatability and less toxiferous. Particularly, the hydrothermal method can obviously accelerate the QDs growth process, namely timesaving. High-quality $CdTe_xSe_{1-x}$ alloyed QDs can be directly synthesized in water by heating a mixed cadmium salt solution with NaHTe and NaHSe in the presence of thiol capping ligands. NaHTe and NaHSe are usually prepared by reduction of Te powder and Na_2SeO_3 powder with $NaBH_4$, respectively. The properties of the ternary alloyed QDs have a great relationship with the composition of the system and the capping ligands. Various strategies aimed for growing QDs with homogeneously alloyed structure have been proposed, for example, an interplay between the concentration ratio of components due to the different reactivity of anion precursors under cadmium-limited reaction conditions [20, 21], or tuning the reactivity of anion precursors through complexation with suitable ligands [22]. The capping ligands used in the synthesis of water-soluble alloyed QDs are mainly thiol ligands, such as thioglycolic acid (TGA), 3-mercaptopropionic acid (MPA) and L-cysteine (L-Cys). TGA and MPA are common stabilizers for water-soluble QDs, but these two thiol ligands are both volatile liquids with an awful odor and MPA carcinogenic property further deters its use from laboratories under stringent safety requirements [23]. L-Cys is an antioxidant and nontoxic chemicals, and also suitable for synthesis of high-quality water-soluble QDs. Up to now, the synthesis of alloyed QDs with L-Cys and its derivatives have seldom been reported.

In this article, high-quality $CdTe_xSe_{1-x}$ alloyed QDs were prepared via a hydrothermal method at low temperature using different capping agents, including MPA and L-Cys. The effect of pH value on the optical properties of the $CdTe_xSe_{1-x}$ QDs was studied. $CdTe_xSe_{1-x}$ QDs with different compositions were prepared to investigate the composition dependence of the optical properties. To enhance the PL efficiency and stability of the $CdTe_xSe_{1-x}$ QDs, CdS inorganic shell was grown on the core through an epitaxial growth process. This hydrothermal method described in this article is also utilizable for the synthesis of other water-soluble QDs. The PL efficiency of the L-Cys-capped $CdTe_xSe_{1-x}$ QDs has to be further improved in the future exploration and would be a potential candidate for applications in fields, such as optoelectronic devices, biological labeling.

Experimental

Chemicals

$CdCl_2 \cdot 2.5H_2O$ (98 %), tellurium powder (Te, 99 %), thioglycollic acid (TGA, 99 %), L-cysteine (L-Cys, 98.5 %), NaOH (96 %) and sodium borohydride ($NaBH_4$, 96 %) were purchased from Shanghai Chemical Reagent Company. Sodium sulfide ($Na_2S \cdot 9H_2O$, 98 %) and Na_2SeO_3 (97 %) were taken from Tianjin Chemical Reagent Institute. 3-mercaptopropionic acid (MPA, 99 %) were supplied by Alfa Aesar. All the chemicals were used directly without any further purification. The pure water was taken from a Milli-Q synthesis system at 18.2 MΩ·cm.

Hydrothermal Synthesis of L-Cys-capped CdTeSe QDs

The synthesis of L-Cys-capped CdTeSe QDs was carried out through a facile hydrothermal method, which was timesaving and economic. Typically, 0.0913 g (0.4 mmol) of $CdCl_2 \cdot 2.5H_2O$ and 0.0738 g (0.6 mmol) of L-Cys were dissolved in 25 mL of pure water, using a ultrasonic cleaner to accelerate the dissolution of L-Cys, followed by the pH adjustment of the solution to 11.5 through dropwised addition of a 2 M NaOH solution. The resulting solution was then degassed by nitrogen to get rid of the infaust oxygen. The Te and Se precursors were prepared by reducing of Te powder and Na_2SeO_3 powder using $NaBH_4$ in water, respectively. In a typical procedure, 0.1-mmol of tellurium powder and 1 mmol of $NaBH_4$ were dissolved in 2 mL pure water with constant stirring and degassed by nitrogen, followed by heating the solution slowly to 60 °C. As the temperature reached 60 °C, the color of the above solution was turned to light-purple. After a few minutes, the black tellurium powder was dissolved and the solution was changed into clearly, indicating the completion of the reaction between Te and $NaBH_4$. Similarly, 0.1 mmol of Na_2SeO_3 were reduced by 1 mmol of $NaBH_4$ in 2 mL pure water at 80 °C degassing by nitrogen, the solution of which would first turn to be erythrine, then colorless. Then the resulting Te and Se precursors were simultaneously injected into the as-prepared Cd^{2+} solution using two syringes with violent stirring at anaerobic condition. Finally, the mixture solution was transferred into a Teflon-lined stainless steel autoclave and maintained at 120 °C for several hours, which can be adjusted in order to obtain various sizes of CdTeSe

alloyed QDs. To fabricate $CdTe_xSe_{1-x}$ QDs with different compositions, the molar ratio of Te-to-Se precursors was changed. $CdTe_xSe_{1-x}$ QDs capped with different ligands were synthesized using analogous procedure.

Encapsulation of $CdTe_xSe_{1-x}$ QDs with CdS Shell

The preparation of $CdTe_xSe_{1-x}$/CdS core-shell QDs is described as follows. All the reaction is performed at an anaerobic condition to avoid the interaction of oxygen. To remove the unreacted chemicals, the original $CdTe_xSe_{1-x}$ core solution was precipitated using 2-propanol mixed with ethanol followed by centrifugation at 5000 rpm and redispersed in adequate pure water. Then adequate quantity of $CdCl_2 \cdot 2.5H_2O$ and TGA were added into the above solution followed by adjusting the pH value to 11.5 using 2 M NaOH under stirring. Next, the resulting solution was added into a four-necked flask and heat-treated to 100 °C with constant stirring under nitrogen flow. Simultaneously, $Na_2S \cdot 9H_2O$ is dissolved in deionized water (0.06 mol/L) bubbled with nitrogen. When the Cd^{2+} solution was heat-treated to 100 °C, the Na_2S solution of 1 mL was injected dropwised through a syringe within 1 min under vigorous stirring. The solution was refluxed at 100 °C for further certain time. To thicken the CdS shell, the Na_2S solution was added for several times at a regular interval of 30 min with the same injection speed.

Characterization

UV–vis absorption and PL spectra of the samples were measured at room temperature using Hitachi U-4100 and F-4600 spectrophotometers, respectively. For absorption and emission measurements, the QDs sample was diluted in adequate pure water. The X-ray powder diffraction (XRD) patterns of samples were recorded using Bruker D8 diffractometer using a Cu Kα target. The transmission electron microscopy (TEM) images of samples were acquired via a JEM-2010 electron microscope. Suitable concentration of QDs solution was deposited on the copper grid with carbon support for obtaining TEM images.

Results and Discussion

The synthesis of ternary alloyed $CdTe_xSe_{1-x}$ QDs described in this article is based on the well-established aqueous synthesis routes for II-VI semiconductor QDs using short-chain thiol as capping ligands. Basically, the precursor solutions of NaHTe and NaHSe were injected simultaneously into the Cd-thiolate solution at alkaline pH and anaerobic condition. Under the presence of excess thiol ligands (L-Cys) and cadmium-rich conditions of our synthetic system, the simultaneous injection of NaHTe and NaHSe resulted in the formation of $CdTe_xSe_{1-x}$ precursors, most probably in form of some water-soluble $(CdTe_xSe_{1-x})$-(L-Cys) complexes [24], which was accompanied by the change of the solution appearance from colorless to orange. After being heat-treated at 120 °C via hydrothermal method, the $CdTe_xSe_{1-x}$ precursors would crystallize and grow to $CdTe_xSe_{1-x}$ alloyed QDs. The growth of $CdTe_xSe_{1-x}$ QDs could be monitored by absorption and PL spectrum.

As it is known to all, MPA is a wonderful capping agents for preparing large-sized water-soluble CdTe QDs with near-infrared emission [23], though the awful and carcinogenic odor have limited its utilization in biological application. For comparison, we prepared MPA-capped CdTe QDs via hydrothermal method, keeping the initial $[CdCl_2]:[NaHTe]:[MPA]$ in the precursor solution to $1:0.5:1.5([CdCl_2])=16$ mM). Both
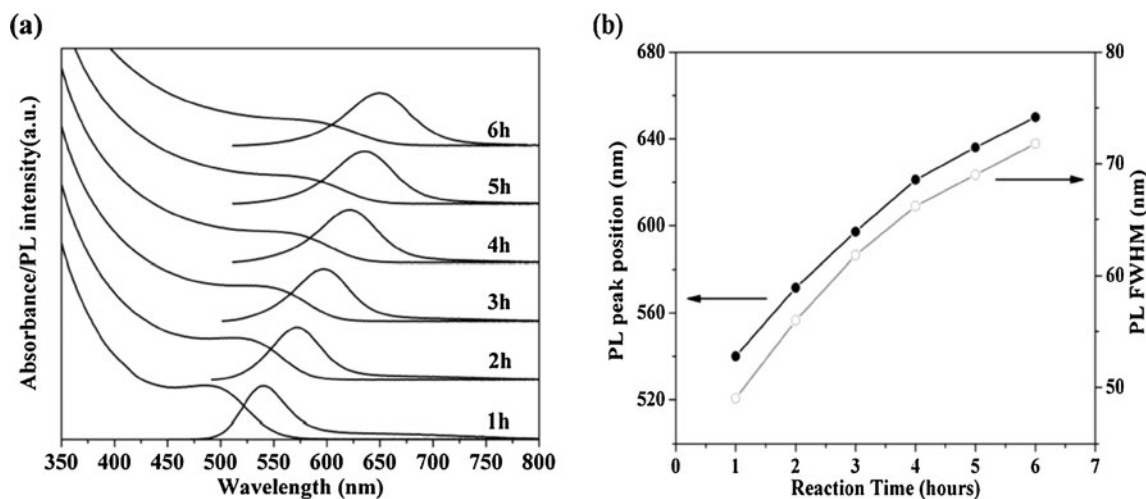

Fig. 1 **a** Temporal evolution of absorption and PL spectra of MPA-capped CdTe QDs during their growth at 120 °C. **b** Variation of PL peak position and fwhm of MPA-capped CdTe QDs versus the reaction time
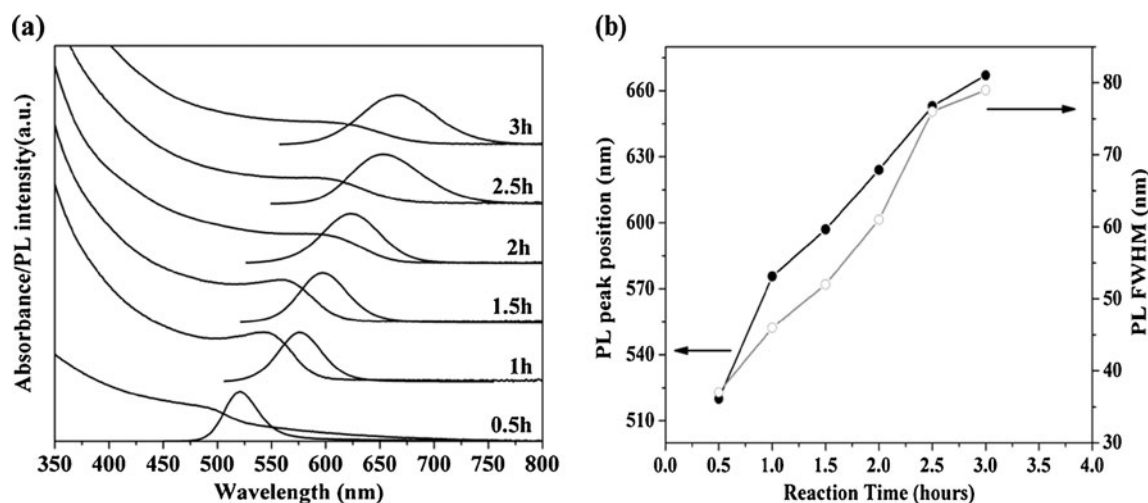
J Fluoresc (2013) 23:1247–1254

Fig. 2 **a** Temporal evolution of absorption and PL spectra of L-Cys-capped CdTeSe (Se/Te=1/10) QDs during their growth at 120 °C. **b** Variation of PL peak position and fwhm of L-Cys-capped CdTeSe (Se/Te=1/10) QDs versus the reaction time

the absorption and PL spectra of the MPA-capped CdTe QDs shifted to longer wavelengths, as the growth time were prolonged for several hours (Fig. 1a). Figure 1b shows the variation of PL peak position and fwhm of MPA-capped CdTe QDs as the reaction time increased from 1 h to 6 h. During the growth process of the QDs, the PL peak of the CdTe QDs red shifted from 540 nm corresponding to the growth time of 1 h to 650 nm corresponding to 6 h, indicating the growth of the CdTe particles. The PL peak of the CdTe QDs might shift to further longer wavelength if the growth time be further prolonged. Figure 1a shows that there is deep-trap emission at the initial growth stage of CdTe QDs, indicating the existence of surface defects [25–27], which might be the reason of the low PL QYs of MPA-capped CdTe QDs. With increasing time, the PL spectra became more symmetrical, together with the enhancement of PL intensity. However, the full width at half maximum (fwhm) of the CdTe QDs also increased

(Fig. 1b) with the prolongation of the reaction time, which might be caused by the Ostwald ripening process [28]. Even so the fwhm (maximum 71 nm, minimum 49 nm) is a relatively small value compared with the ones published in last literature, revealing the narrow size distribution of our CdTe QDs.

L-Cys is a nontoxic capping agents for QDs, having been reported by several groups [23]. In this article, we also prepared L-Cys-capped CdTe$_x$Se$_{1-x}$ QDs via hydrothermal method. We found that the PL intensity and stability of L-Cys-capped CdTe$_x$Se$_{1-x}$ QDs were higher than that stabilized by MPA. Figure 2a shows the absorption and PL spectra of L-Cys-capped CdTe$_x$Se$_{1-x}$ QDs with the prolongation of the reaction time from 0.5 h to 3 h. The detailed information about the PL peak position and fwhm of PL spectra are presented in Fig. 2b. As the reaction time increased from 0.5 h to 3 h, the PL peak red shifted from 520 nm to 667 nm,
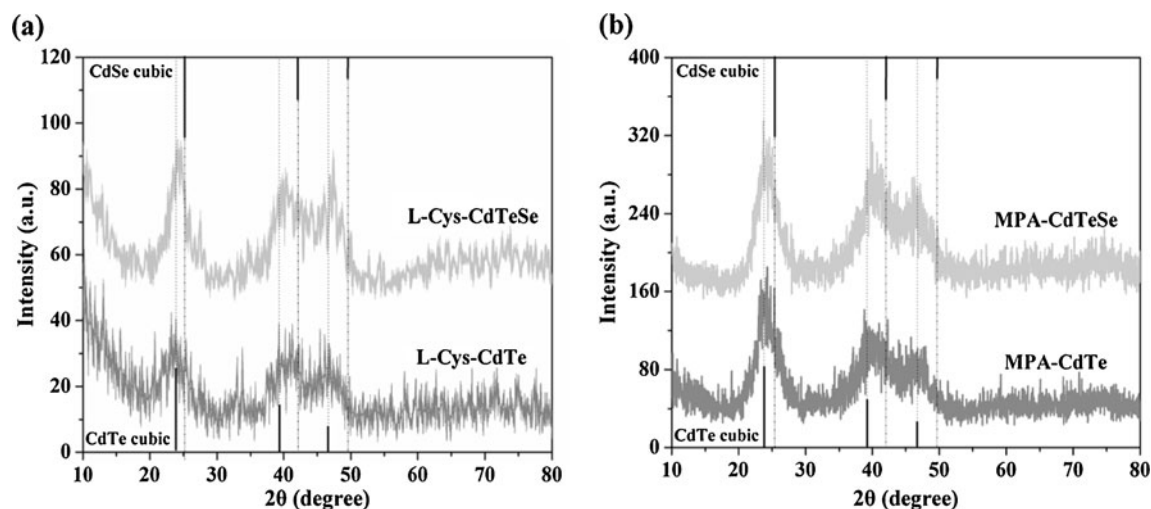

Fig. 3 **a** Powder X-ray diffraction patterns of L-Cys-capped CdTe and CdTeSe (Se/Te=1/10) QDs. **b** Powder X-ray diffraction patterns of MPA-capped CdTe and CdTeSe (Se/Te=1/10) QDs

together with the broadening of the PL fwhm. As readily seen in Fig. 2a, a strong luminescence band is observed near the band edge of the CdTe$_x$Se$_{1-x}$ QDs and no deep trap emission is detected, indicating the decent emissive properties of the QDs [25–27]. On the basis of plenty of experiments, we found that L-Cys is more suitable for growth of high-quality CdTe$_x$Se$_{1-x}$ QDs than MPA through hydrothermal method. The reason might be related to the chemical nature of the two thiol ligands. Compared with MPA, L-Cys has a NH$_2$ group bonding to the middle carbon atom. The NH$_2$ group might affect the reactivity of L-Cys, resulting in the effective encapsulation of L-Cys to the surface of the CdTe$_x$Se$_{1-x}$ core. It seems that thiol ligands can conjunct with the surface of the CdTe$_x$Se$_{1-x}$ QDs via the Cd-S bond. The Cd-S bond between L-Cys and CdTe$_x$Se$_{1-x}$ QDs might be stronger than that of MPA and CdTe$_x$Se$_{1-x}$ QDs, which might be related to the chemical nature of MPA and L-Cys, leading to the high-quality of the L-Cys-capped CdTe$_x$Se$_{1-x}$ QDs.

One of the advantages of the hydrothermal method is that it allows the reaction process to take place at high temperature. Thus the growth rate of the QDs would be faster than traditional aqueous routes, which may introduce more surface defects to the QDs, leading to the low PL efficiency of the CdTe$_x$Se$_{1-x}$ QDs. In addition, high temperature can cause the decomposition of the thiol ligands, reported by several groups [23, 29, 30], which will release reactive S atoms, triggering the formation of CdS shell on the surface of the CdTe$_x$Se$_{1-x}$ core. In our experiments, there is no indication for the formation of CdS shell, which can be deduced from the powder XRD patterns of CdTe$_x$Se$_{1-x}$ QDs (Fig. 3). The XRD patterns of MPA-capped CdTe$_x$Se$_{1-x}$ QDs (Fig. 3b) are well consistent with that of bulk cubic CdTe structure (JCPDS 15–0770), with no signs of CdS diffraction peaks in the curve, indicating that the resulting CdTe$_x$Se$_{1-x}$ QDs are pure CdTe core. Similarly, L-Cys-capped CdTe$_x$Se$_{1-x}$ QDs are also cubic CdTe structure, inferred from the three diffraction peaks of (111), (220) and (311) in Fig. 3a. The weak diffraction peaks at about

Table 1 PL peak wavelength and fwhm of PL spectra of L-Cys-capped CdTe$_x$Se$_{1-x}$ QDs with different Se-to-Te molar ratios

Se/Te molar ratio	PL peak wavelength (nm)	FWHM (nm)
1/10	666.5	61
2/10	655.8	59
3/10	624	52
4/10	621.8	48
5/10	617.8	56.5

34° in Fig. 3a was caused by the stacking defects in CdTe nanocrystals, indicating that hexagonal CdTe structure doped in a main cubic structure. The result in Fig. 3 indicates that the XRD patterns of CdTeSe (Se/Te molar ratio of 1/10) QDs are similar to that of CdTe QDs, but slightly shift towards large angle, at least indicating that both Te and Se elements are the components of the resulting QDs. The structure of the resultant QDs might be core-shell structure or alloyed composition. In order to confirm the structure of the resultant QDs, we also adjusted the molar ratio of Se-to-Te to prepare CdTe$_x$Se$_{1-x}$ QDs of different composition.

The molar ratios of Se-to-Te upon preparation was changed from 1/10 to 5/10 to investigate the composition dependence of the optical properties of CdTe$_x$Se$_{1-x}$ QDs. Figure 4 shows the variation of PL spectra of L-Cys-capped CdTe$_x$Se$_{1-x}$ QDs versus the molar ratio of Se-to-Te changing from 1/10 to 5/10. The detailed information about the PL peak wavelength and the fwhm of PL spectra is demonstrated in Table 1. The PL peak of the CdTe$_x$Se$_{1-x}$ QDs was shifted to short wavelength as the percentage composition of Se increase. This phenomenon can be an evidence for the alloyed composition of the resultant CdTe$_x$Se$_{1-x}$ QDs. If the resulting QDs have core-shell structure, the PL peak will be red shifted with increasing the amount of Se, as the CdSe shell thickens. Thus, the CdTe$_x$Se$_{1-x}$ QDs prepared in our experiments are more inclined to alloyed composition.
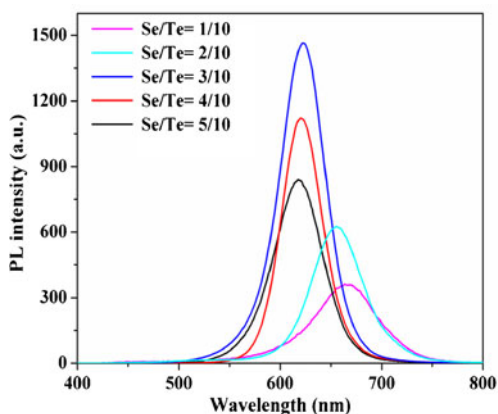

Fig. 4 PL spectra of L-Cys-capped CdTe$_x$Se$_{1-x}$ QDs with different Se-to-Te molar ratios. The molar ratios of Se-to-Te changes from 1/10 to 5/10
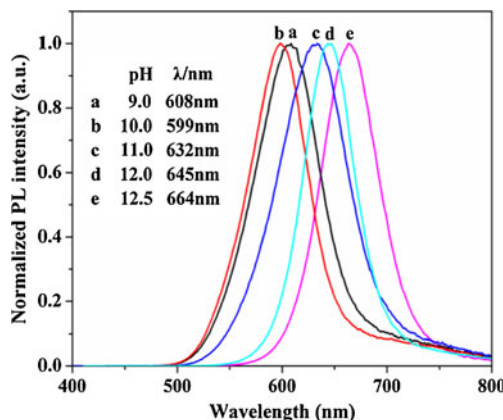

Fig. 5 Normalized PL spectra of L-Cys-capped CdTeSe (Se/Te=1/10) QDs prepared at different pH conditions
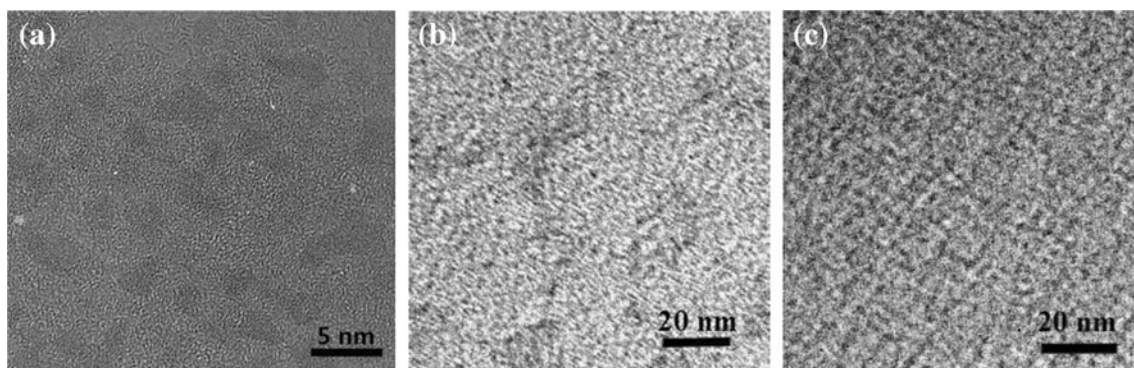
Fig. 6 TEM images of L-Cys-capped CdTe QDs (**a**), L-Cys-capped CdTeSe (Se/Te=1/10) QDs (**b**), and TGA-capped CdTeSe/CdS core-shell QDs (**c**)

Common alloyed semiconductor QDs typically show linear changes of band gap and, correspondingly, of optical properties with the changing of the composition. The deviation from this phenomenon, denoted as optical bowing effect [31], has been modeled by Zunger and coworkers [31, 32]. The CdTe$_x$Se$_{1-x}$ QDs described here also showed linear changes of optical properties with composition, as can be seen from Table 1. The PL peak wavelength, correspondingly to bandgap of the CdTe$_x$Se$_{1-x}$ QDs, and composition had a linear relationship, also confirming the alloyed composition of the CdTe$_x$Se$_{1-x}$ QDs. The variation of PL fwhm of the alloyed CdTe$_x$Se$_{1-x}$ QDs with composition is also investigated through a series of experiments. However, the PL fwhm and composition didn't show linear relationship (Table 1), indicating that the PL fwhm of the QDs had less dependence on the composition. The PL quantum yields of the alloyed CdTeSe QDs with different composition are in the range of 10 %–20 %, which is relatively low compared to the QDs synthesized in organic phase. As the molar ratio of Se-to-Te changed from 1/10 to 5/10, the PL quantum yields of the alloyed CdTeSe QDs firstly increased then decreased. When the molar ratio of Se-to-Te was 3/10, the PL quantum yield

reached the highest 19.2 %. Thus, we can see that composition can influence the optical properties of the alloyed CdTeSe QDs.

In this article, we also investigated the pH value of the reaction solution on the growth kinetics of the alloyed CdTe$_x$Se$_{1-x}$ QDs. As we can see from Fig. 5, the PL peak wavelength of the CdTeSe (Se/Te molar ratio of 1/10) QDs shifts to longer wavelength as the pH value of the reaction solution increases from 9.0 to 12.5, except for pH=10. The general trend can be concluded that PL peak wavelength and pH value of the reaction solution had a positive correlation, because the PL peak wavelength at pH values of 9.0 and 10.0 (Fig. 5) are very close in with each. The PL peak wavelength or band gap of the CdTeSe (Se/Te molar ratio of 1/10) QDs is determined by the particle size of the QDs. Therefore, the growth rate of the QDs became faster at a high pH value. Thus, the PL wavelength of resulting QDs was red-shifted. Though this inference is lack of theoretical evidence, it is really a good exploration on the preparation conditions of the CdTe$_x$Se$_{1-x}$ QDs and we will further explore on this field.

The typical TEM images of the as-prepared L-Cys-capped CdTe and CdTeSe (Se/Te molar ratio of 1/10) QDs are
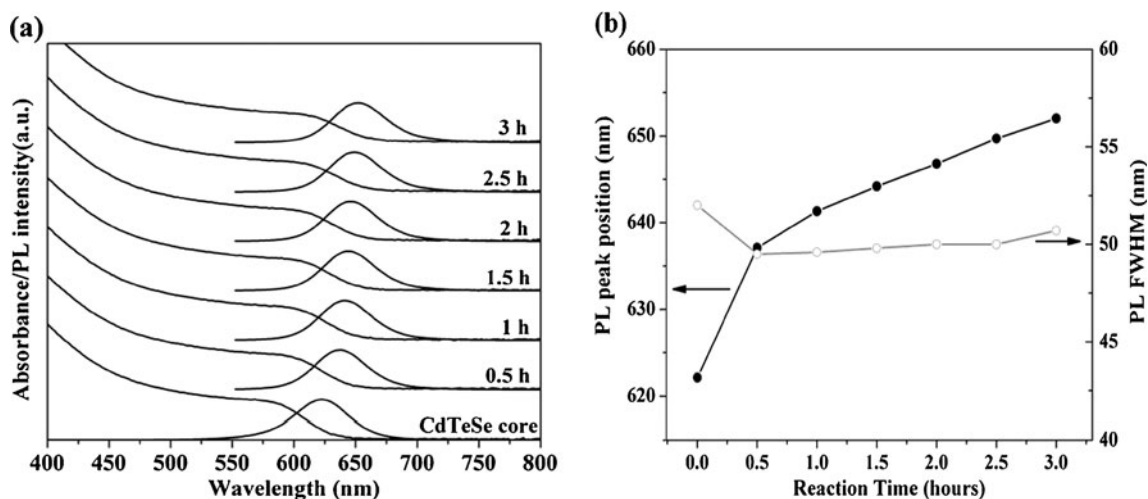

Fig. 7 **a** Temporal evolution of absorption and PL spectra of CdTeSe (Se/Te=1/10) core and CdTeSe/CdS core-shell QDs as the shell growth time increased from 0.5 h to 3 h. **b** Variation of PL peak position and fwhm of CdTeSe/CdS core-shell QDs versus the reaction time

depicted in Fig. 6. It is quite evident that these QDs are close to spherical dots with excellent monodispersity. As we estimated from Fig. 6, the average diameter of the CdTe QDs is about 2.2 nm, which is slightly smaller than the CdTeSe QDs. The CdTe and CdTeSe (Se/Te molar ratio of 1/10) QDs used for TEM observation were prepared at same reaction condition, and the content of anions was also identical. The only distinction is that the reactivity of Se precursor (NaHSe) are higher than that of Te (NaHTe) [33], resulting in a higher growth rate of the CdTeSe QDs than that of CdTe QDs. Thus the particle size of the resultant CdTeSe QDs was larger than that of CdTe QDs.

In order to improve the PL intensity and stability of the $CdTe_xSe_{1-x}$ QDs, a CdS inorganic shell was coated on the CdTeSe (Se/Te molar ratio of 1/10) core through epitaxial growth. Figure 7a shows the absorption and PL spectra of CdTeSe/CdS core-shell QDs as the reaction time increased from 0.5 h to 3 h. Detailed information about the PL peak position and fwhm of the CdTeSe/CdS QDs with time are shown in Fig. 7b. As the reaction time increased, both the absorption and PL spectra were shifted to longer wavelength. On increasing time to 3 h, the PL spectra exhibited a red shift of about 31 nm in respect to that of CdTeSe core, indicating the leakage of excitons into the shell layers. In Fig. 7b, the PL fwhm of CdTeSe/CdS core-shell QDs revealed a slight decrease as the reaction time increase, which indicated that the size distribution of the resultant core-shell QDs were still very good after encapsulation. Figure 7 shows that the peaks of pure CdS QDs were not observed in either the absorption or the PL spectra of CdTeSe/CdS core-shell QDs, indicating that pure CdS QDs are not formed after adding the Na_2S solution to initial the shell growth. A typical TEM image of CdTeSe/CdS core-shell QDs is shown in Fig. 6c. The morphology of the CdTeSe/CdS QDs is also spherical dots and the size distribution of these QDs is still very good after encapsulation. The stability of the CdTeSe/CdS QDs was greatly enhanced compared with the CdTeSe core. The CdTeSe/CdS core-shell QDs can be stored for six months without loss of the emission intensity.

Conclusions

High-quality thiol-stabilized $CdTe_xSe_{1-x}$ alloyed QDs were prepared via a facile hydrothermal method at low temperature. Through plenty of experiments, we found that the PL properties of the L-Cys-capped $CdTe_xSe_{1-x}$ QDs are better than those of MPA-capped $CdTe_xSe_{1-x}$ QDs. Composition of the $CdTe_xSe_{1-x}$ QDs were adjusted to investigate the composition dependence of the optical properties. PL peak wavelengths of the alloyed $CdTe_xSe_{1-x}$ QDs were found to be blue shift as the percentage composition of the Se element in the whole anions increase. We also investigated the effect of pH value of the reaction solution on the growth kinetics of the $CdTe_xSe_{1-x}$ QDs. After being coated with a CdS shell, PL properties and stability of the $CdTe_xSe_{1-x}$ QDs were greatly enhanced.

References

1. Anderson RE, Chan WCW (2008) Systematic investigation of preparing biocompatible, single, and small ZnS-capped CdSe quantum dots with amphiphilic polymers. ACS Nano 2(7):1341–1352
2. Murray CB, Norris DJ, Bawendi MG (1993) Synthesis and characterization of nearly monodisperse CdE (E=S, Se, Te) semiconductor nanocrystallites. J Am Chem Soc 115(19):8706–8715
3. Burda C, Chen XB, Narayanan R, El-Sayed MA (2005) Chemistry and properties of nanocrystals of different shapes. Chem Rev 105(4):1025–1102
4. Chan WCW, Nie S (1998) Quantum dot bioconjugates for ultrasensitive nonisotopic detection. Science 281(5385):2016–2018
5. Dabbousi BO, Rodriguez-Viejo J, Mikulec FV, Heine JR, Mattoussi H, Ober R, Jensen KF, Bawendi MG (1997) (CdSe)ZnS core-shell quantum dots: synthesis and characterization of a size series of highly luminescent nanocrystallites. J Phys Chem B 101(46):9463–9475
6. Zhang Y, Li Y, Yan XP (2009) Photoactivated CdTe/CdSe quantum dots as a near infrared fluorescent probe for detecting biothiols in biological fluids. Anal Chem 81(12):5001–5007
7. Seo H, Kim S (2007) In situ synthesis of CdTe/CdSe core-shell quantum dots. Chem Mater 19(11):2715–2717
8. Liao L, Zhang H, Zhong X (2011) Facile synthesis of red- to near-infrared-emitting CdTexSe1-x alloyed quantum dots via a noninjection one-pot route. J Lumin 131(2):322–327
9. Jr MB, Moronne M, Gin P, Weiss S, Alivisatos AP (1998) Semiconductor nanocrystals as fluorescent biological labels. Science 281(5385):2013–2016
10. Dubertret B, Skourides P, Norris DJ, Noireaux V, Brivanlou AH, Libchaber A (2002) In vivo imaging of quantum dots encapsulated in phospholipid micelles. Science 298(5599):1759–1762
11. Pal BN, Ghosh Y, Brovelli S, Laocharoensuk R, Klimov VI, Hollingsworth JA, Htoon H (2012) 'Giant' CdSe/CdS core/shell nanocrystal quantum dots as efficient electroluminescent materials: strong influence of shell thickness on light-emitting diode performance. Nano Lett 12(1):331–336
12. Blackman B, Battaglia D, Peng X (2008) Bright and water-soluble near IR-emitting CdSe/CdTe/ZnSe type-II/type-I nanocrystals, tuning the efficiency and stability by growth. Chem Mater 20(15):4847–4853
13. Chon B, Bang J, Park J, Jeong C, Choi JH, Lee J, Joo T, Kim S (2011) Unique temperature dependence and blinking behavior of CdTe/CdSe (core/shell) type-II quantum dots. J Phys Chem C 115(2):436–442
14. Wang R, Calvignanello O, Ratcliffe CI, Wu X, Leek DM, Zaman MB, Kingston D, Ripmeester JA, Yu K (2009) Homogeneously-alloyed CdTeSe single-sized nanocrystals with bandgap photoluminescence. J Phys Chem C 113(9):3402–3408

15. Pons T, Lequeux N, Mahler B, Sasnouski S, Fragola A, Dubertret B (2009) Synthesis of near-infrared-emitting, water-soluble CdTeSe/CdZnS core/shell quantum dots. Chem Mater 21(8):1418–1424

16. Korgel BA, Monbouquette HG (2000) Controlled synthesis of mixed core and layered (Zn, Cd)S and (Hg, Cd)S nanocrystals within phosphatidylcholine vesicles. Langmuir 16(8):3588–3594

17. Harrison MT, Kershaw SV, Burt MG, Eychmuller A, Weller H, Rogach AL (2000) Wet chemical synthesis and spectroscopic study of CdHgTe nanocrystals with strong near-infrared luminescence. Mater Sci Eng B 69(2):355–360

18. Zhong X, Feng Y, Knoll W, Han M (2003) Alloyed ZnxCd1-xS nanocrystals with highly narrow luminescence spectral width. J Am Chem Soc 125(44):13559–13563

19. Zhong X, Zhang Z, Liu S, Han M, Knoll W (2004) Embryonic nuclei-induced alloying process for the reproducible synthesis of blue-emitting ZnxCd1-xSe nanocrystals with long-time thermal stability in size distribution and emission wavelength. J Phys Chem B 108(40):15552–15559

20. Bailey RE, Nie S (2003) Alloyed semiconductor quantum dots: tuning the optical properties without changing the particle size. J Am Chem Soc 125(23):7100–7106

21. Jiang W, Singhal A, Zheng J, Wang C, Chan WCW (2006) Optimizing the synthesis of red- to near-IR-emitting CdS-capped CdTexSe1-x alloyed quantum dots for biomedical imaging. Chem Mater 18(20):4845–4854

22. Swafford LA, Weigand LA, Bowers MJ, McBride JR, Rapaport JL, Watt TL, Dixit SK, Feldman LC, Rosenthal SJ (2006) Homogeneously alloyed CdSxSe1-x nanocrystals: synthesis, characterization, and composition/size-dependent band gap. J Am Chem Soc 128(37):12299–12306

23. Zhao D, He Z, Chan WH, Choi MMF (2009) Synthesis and characterization of high-quality water-soluble near-infrared-emitting CdTe/CdS quantum dots capped by N-acetyl-L-cysteine via hydrothermal method. J Phys Chem C 113(4):1293–1300

24. Shavel A, Gaponik N, Eychmuller A (2006) Factors governing the quality of aqueous CdTe nanocrystals: calculations and experiment. J Phys Chem B 110(39):19280–19284

25. Kapitonov AM, Stupak AP, Gaponenko SV, Petrov EP, Rogach AL, Eychmuller A (1999) Luminescence properties of thiol-stabilized CdTe nanocrystals. J Phys Chem B 103(46):10109–10113

26. Wuister SF, Koole R, Donega CM, Meijerink A (2005) Temperature-dependent energy transfer in cadmium telluride quantum dot solids. J Phys Chem B 109(12):5504–5508

27. Osovsky R, Kloper V, Kolny-Olesiak J, Sashchiuk A, Lifshitz E (2007) Optical properties of CdTe nanocrystal quantum dots, grown in the presence of Cd^0 nanoparticles. J Phys Chem C 111(29):10841–10847

28. Talapin DV, Rogach AL, Shevchenko EV, Kornowski A, Haase M, Weller H (2002) Dynamic distribution of growth rates within the ensembles of colloidal II-VI and III-V semiconductor nanocrystals as a factor governing their photoluminescence efficiency. J Am Chem Soc 124(20):5782–5790

29. Rogach AL (2000) Nanocrystalline CdTe and CdTe(S) particles: wet chemical preparation, size-dependent optical properties and perspectives of optoelectronic applications. Mater Sci Eng B 69(1):435–440

30. Mao W, Guo J, Yang W, Wang C, He J, Chen J (2007) Synthesis of high-quality near-infrared-emitting CdTeS alloyed quantum dots via the hydrothermal method. Nanotechnology 18(49):485611–485617

31. Bernard JE, Zunger A (1986) Optical bowing in zinc chalcogenide semiconductor alloys. Phys Rev B 34(8):5992–5995

32. Wei SH, Zhang SB, Zunger A (2000) First-principles calculation of band offsets, optical bowings, and defects in CdS, CdSe, CdTe, and their alloys. J Appl Phys 87(3):1304–1311

33. Piven N, Susha AS, Doblinger M, Rogach AL (2008) Aqueous synthesis of alloyed CdSexTe1-x nanocrystals. J Phys Chem C 112(39):15253–15259